



## Original Article

Monitoring real time polymorphic transformation of sulfanilamide by diffuse reflectance visible spectroscopy<sup>☆</sup>Tracy O. Ehiwe<sup>a</sup>, Bruce D. Alexander<sup>a</sup>, John C. Mitchell<sup>a,\*</sup>, Martin J. Snowden<sup>a</sup>, Laura J. Waters<sup>b</sup><sup>a</sup> Medway Centre for Formulation Science, Faculty of Engineering and Science, University of Greenwich at Medway, Chatham Maritime, Kent ME4 4TB, UK<sup>b</sup> School of Applied Sciences, University of Huddersfield, Queensgate, Huddersfield HD1 3DH, UK

## ARTICLE INFO

## Article history:

Received 31 July 2015

Received in revised form

17 December 2015

Accepted 18 December 2015

## Keywords:

Polymorphic transformation

Sulfanilamide

Diffuse reflectance visible spectroscopy

Powder X-ray diffraction

Differential scanning calorimetry

## ABSTRACT

This study investigated the development of a novel approach to surface characterization of drug polymorphism and the extension of the capabilities of this method to perform 'real time' in situ measurements. This was achieved using diffuse reflectance visible (DRV) spectroscopy and dye deposition, using the pH sensitive dye, thymol blue (TB). Two polymorphs, SFN- $\beta$  and SFN- $\gamma$ , of the drug substance sulfanilamide (SFN) were examined. The interaction of adsorbed dye with polymorphs showed different behavior, and thus reported different DRV spectra. Consideration of the acid/base properties of the morphological forms of the drug molecule provided a rationalization of the mechanism of differential coloration by indicator dyes. The kinetics of the polymorphic transformation of SFN polymorphs was monitored using treatment with TB dye and DRV spectroscopy. The thermally-induced transformation fitted a first-order solid-state kinetic model ( $R^2=0.992$ ), giving a rate constant of  $2.43 \times 10^{-2} \text{ s}^{-1}$ .

© 2016 Xi'an Jiaotong University. Production and hosting. Published by Elsevier B.V. This is an open access article under the CC BY-NC-ND license (<http://creativecommons.org/licenses/by-nc-nd/4.0/>).

## 1. Introduction

Polymorphic transformations can have a significant influence on the processing and storage of crystalline powders. Change in crystalline structure affects the therapeutic effectiveness and stability of drug products; therefore, the ability to monitor the effect of process stages on drug polymorphic transformation is crucial in drug manufacture [1]. The transformation from one polymorphic form to another can be thermally, mechanically or moisture-induced.

Solid-state phase (polymorphic) transformations are generally based on overlapping mechanisms of nucleation, growth and impingement [2,3]. Solid-state kinetic evaluation typically involves modeling the fraction transformed as a function of time.

Eq. 1 represents a generic integral rate equation for solid-state kinetics:

$$g(a) = kt \quad (1)$$

where  $g$  is a function of the extent of reaction,  $a$  is the fraction of phase transformed or extent of growth of new phase,  $k$  is the rate constant, and  $t$  is time. The kinetics of the phase transformation is heterogeneous in nature, which suggests that several factors affect the kinetics of transformation including activation

energy of nucleation and growth, difference in the crystal imperfections, particle size and particle morphology, and variation in growth rate along crystallographic axes. These factors contribute to the development of different models used in the characterization of the kinetics of solid-state phase transformation resulting in acceleratory, deceleratory, linear or sigmoidal shapes for their respective isothermal  $\alpha$ -time curves [3,4].

A variety of techniques have been employed to characterize the kinetics of polymorphic transformation in situ. Examples include near infrared spectroscopy (NIR) [5,6], vibrational spectroscopy [7,8], powder X-ray diffraction (PXRD) [9] and temperature-controlled simultaneous small/wide angle X-ray scattering [10]. Previous reports also include the study of the thermodynamics of the conversion of sulfanilamide (SFN) polymorphs by energy dispersive X-ray diffraction [11]. Monitoring processes, especially by in situ methods including diffuse reflectance visible (DRV) spectroscopy, offer a better understanding of the intrinsic properties of systems, thus improving process control [12].

This study reports on a novel 'real time' method for monitoring thermally induced conversion of polymorphs using DRV spectroscopy and kinetic evaluation of the generated data. Polymorphs of SFN were examined. The two polymorphs (SFN- $\beta$  and SFN- $\gamma$ ) studied are enantiotropically related and the conversion of SFN- $\beta$  to SFN- $\gamma$  can be induced at elevated temperatures. Although other reports on the analysis of polymorphs include the use of NIR [5,6] and vibrational spectroscopy [7,8], we have used DVR spectroscopy as the technique of choice for this study. We have

<sup>☆</sup>Peer review under responsibility of Xi'an Jiaotong University.

\* Corresponding author.

E-mail address: [J.Mitchell@Greenwich.ac.uk](mailto:J.Mitchell@Greenwich.ac.uk) (J.C. Mitchell).

experience in using DRV spectroscopy for the differentiation of crystalline and amorphous forms of carbohydrate pharmaceutical excipients, and in this study, we explored the extension of the sensitivity, simplicity of operation and ease of data analysis of this technique to more complex active pharmaceutical ingredients. Furthermore, initial attempts to monitor polymorphic inter-conversion using Raman spectroscopy was proved ineffectively.

## 2. Experimental

### 2.1 Chemicals and preparation

SFN- $\beta$  was prepared by recrystallization in water. Commercial sulfanilamide (> 99.0%) from Sigma Aldrich (Dorset, England) was dissolved in hot water (at 100 °C) and left to cool to ambient temperature (23.5 °C). SFN- $\beta$  was filtered under suction and dried over calcium chloride in a desiccator. SFN- $\gamma$  was obtained from recrystallized SFN- $\beta$  that was heated at 140 °C for 2 h. All polymorphs were stored in a desiccator over calcium chloride (0% RH) prior to analysis to eliminate moisture-induced transformations.

### 2.2 Instrumentation

Philips PW1729 Powder X-ray diffractometer experiments were carried out with a PW1050 goniometer (Lelyweg, Netherlands). Differential scanning calorimetry (DSC) was performed on a Mettler Toledo FP85 DSC system (Greifensee, Sweden). Raman spectroscopy was carried out on a Thermo-Nicolet NXR FT-Raman 9610 spectrometer (Wisconsin, USA). DRV spectroscopy was performed on a Hewlett-Packard 8453 photodiode Array UV-vis Spectrophotometer (California, USA) equipped with a Labsphere RSA-HP-8453 diffuse reflectance accessory (Illinois, USA). Hot-stage microscopy was performed using a Leica optical microscope (Wetzlar, Germany) fitted with a Mettler FP52 hot stage apparatus (Greifensee, Switzerland).

Single crystal data for all polymorphs obtained from the Cambridge Crystal Structural Database (CCSD Codes, SFN  $\beta$  SULAMD03 [13] and SFN  $\gamma$  SULAMD02 [14]) were imputed into the Reflex module of Materials Studio 5.0 software program from Accelrys (San Diego, USA) to obtain simulated powder X-ray data and Miller indices for all reflections.

A full description of the DRV spectroscopy methodology can be found in a previous report by Major, et al. [15].

## 3. Results and discussion

### 3.1 Preparation and characterization of SFN- $\beta$ and SFN- $\gamma$ polymorphs and SFN- $\beta$ -TB and SFN- $\gamma$ -TB

In this study two polymorphs of SFN were examined. The two polymorphs, SFN- $\beta$  and SFN- $\gamma$  studied, are enantiotropically related and the conversion of SFN- $\beta$  to SFN- $\gamma$  can be induced at elevated temperatures, making them good candidates for 'real time' polymorphic interconversion.

The two polymorphs of SFN ( $\beta$  and  $\gamma$  forms) were prepared and analyzed using X-ray diffraction and scanning calorimetry. Four polymorphs of SFN have been recorded, but  $\beta$  and  $\gamma$  are more accessible. The  $\beta$  form is the most stable form under ambient conditions.

The experimental and simulated PXRD patterns for SFN- $\beta$  and SFN- $\gamma$  polymorphs are shown in Fig. 1. The PXRD patterns are different and show defined and sharp peaks which are indicative of their crystalline nature. Experimental 2theta angles agree within  $\pm 0.20^\circ$  of simulated data confirming polymorphic purity;

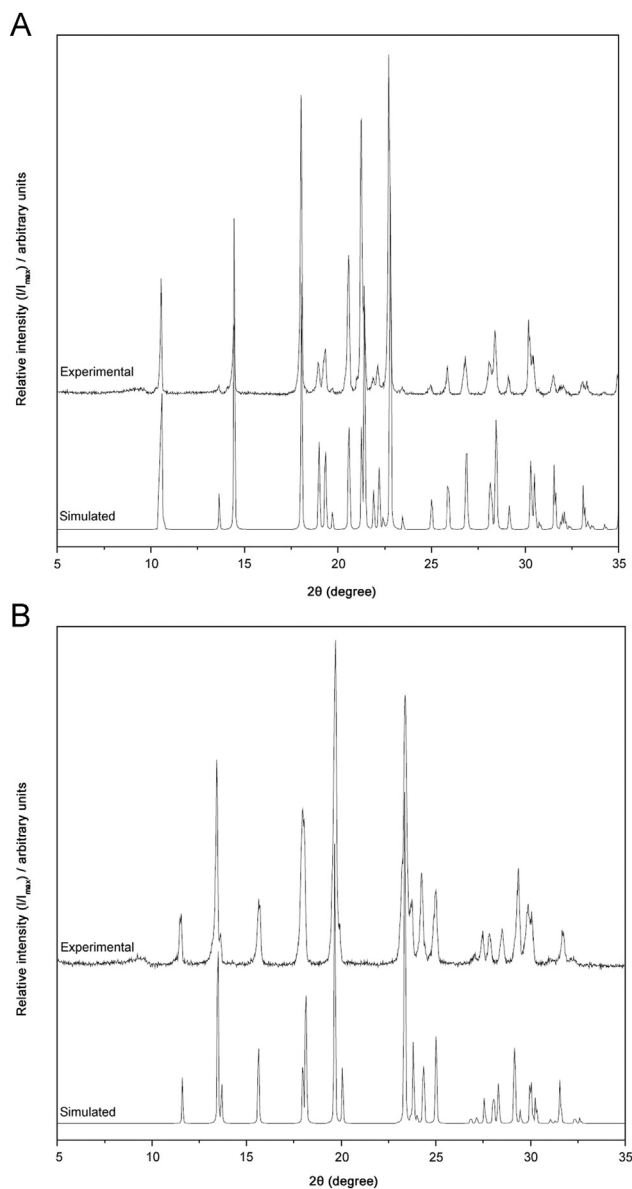


Fig. 1. PXRD patterns for (A) SFN- $\beta$  and (B) SFN- $\gamma$ .

however, peak intensities vary significantly as a result of preferred orientation of several atomic planes to incident X-ray beam.

The thermal behaviors of SFN polymorphs were also analyzed. DSC-thermograms show a single endothermic event for SFN- $\gamma$  ( $T_f = 162.3 \pm 0.3$  °C and  $\Delta H_f = 146.0 \pm 1.0$  J/g) attributed to melting. However, three endothermic transitions  $T_f = 128.3 \pm 1.3$  °C,  $\Delta H_f = 6.9 \pm 3.0$  J/g;  $T_f = 156.0 \pm 1.3$  °C,  $\Delta H_f = 1.33 \pm 0.5$  J/g; and  $T_f = 162.3 \pm 0.3$  °C,  $\Delta H_f = 121.0 \pm 3.5$  J/g, were observed for SFN- $\beta$  attributable to incomplete  $\beta \rightarrow \gamma$  transformation, melting of residual SFN- $\beta$  and melting of SFN- $\gamma$ , respectively.

Dye deposition was achieved using drop-wise addition of 1 mL of methanolic dye solution (200 mg/L) of thymol blue (TB) directly onto 2 g of solid carefully homogenized using a spatula and dried. The typical amount of dye adsorbed per gram of solid was 0.1 mg, which corresponds to the limit of detection of adsorbed dye by the DRV instrument for most of the investigated polymorphic systems. Three separate sample preparations and DRV spectroscopic measurements were conducted for each polymorph. SFN- $\beta$  was always air-dried as oven-drying sometimes introduced SFN- $\gamma$  impurity. For SFN- $\gamma$ , dye deposition was achieved by heating dye treated SFN- $\beta$  to a temperature of 125 °C for 30 min. This heat-induced

transformation method is suitable for SFN- $\gamma$ , because it is prone to solvent-induced polymorphic transformation to SFN- $\beta$ .

The SFN- $\beta$ -TB and SFN- $\gamma$ -TB were characterized by PXRD and DSC to confirm polymorphic form and also to ensure that crystalline integrity was maintained after dye treatment. The samples were screened using sieves to determine particle distribution; whereby the majority had particle size values greater than 450  $\mu\text{m}$ .

PXRD patterns for SFN- $\beta$  treated with TB were compared to the untreated polymorph. Peaks at 2theta values of 10.55, 14.43, 20.57, 21.24 and 22.72 agreed within  $\pm 0.20^\circ$  of untreated data. DSC thermograms of SFN- $\beta$ -TB samples were also analyzed. Dye treated samples indicated only two events, i.e., the  $\beta \rightarrow \gamma$  transformation ( $T_f = 129.0 \pm 0.5^\circ\text{C}$  and  $\Delta H_f = 9.6 \pm 1.0\text{ J/g}$ ) and the melting of SFN- $\beta$  ( $T_f = 162.4 \pm 0.5^\circ\text{C}$  and  $\Delta H_f = 143 \pm 1.0\text{ J/g}$ ).

PXRD patterns for SFN- $\gamma$  treated with TB were likewise compared with the untreated polymorph. Peaks at 2theta values of 11.55, 13.43, 19.69, 24.25 and 29.36 agreed within  $\pm 0.20^\circ$  of untreated data. DSC thermograms of SFN- $\gamma$  treated with TB were again compared to the untreated polymorph. A single endothermic melting was observed for all samples. The onset temperature ( $T_f$ ) and enthalpy of fusion ( $\Delta H_f$ ) were  $T_f = 162.6 \pm 0.5^\circ\text{C}$  and  $\Delta H_f = 144.0 \pm 1.0\text{ J/g}$  for SFN- $\gamma$ -TB.

### 3.2 Isothermal kinetic studies of SFN- $\beta$ transformation monitoring by DRV

TB is a pH sensitive indicator normally used in solution. It contains two ionizable groups, i.e., a sulfonic acid group with a pKa of 1.6 and a phenolic group with a pKa of 8.8. Solution TB can exist as either a neutral species with a  $\lambda_{\text{max}}$  of 547 nm, a mono-anionic form with a  $\lambda_{\text{max}}$  of 434, or as a di-anionic form with a  $\lambda_{\text{max}}$  of 598. These forms of TB are clearly distinguishable by ultraviolet spectroscopy. SFN possesses two ionizable functional groups, i.e., the basic phenyl amine group  $-\text{NH}_2$  (pKa  $1.85 \pm 0.10$ ) and sulfonamide  $-\text{SONH}_2$  group which acts as a weak acid (pKa  $10.10 \pm 0.10$ ), which can play a dominant role in dye deprotonation. The amine group is a stronger base than the sulfonamide group, so the deprotonation of dye molecules is greatly influenced by the surface accessibility of  $-\text{NH}_2$ . The packing motif for both polymorphs may provide insight into the higher basicity of SFN- $\gamma$ . The DRV spectra of the polymorphs of SFN treated with TB indicator are shown in Fig. 2. SFN- $\gamma$ -TB absorbs at  $\lambda_{\text{max}}$  454 nm and 604 nm which are indicative of the yellow mono-deprotonated and blue di-deprotonated species of the dye, respectively. Yellow SFN- $\beta$ -TB absorbs at 454 nm only, suggesting adsorbed mono-anionic TB. Values recorded are red shifted to solution values. It appears that the deprotonation of adsorbed dye molecules is more extensive for SFN- $\gamma$  compared to SFN- $\beta$ , i.e., the proportion of adsorbed  $\text{TB}^{2-}$  is greater for SFN- $\gamma$ , suggesting that SFN- $\gamma$  has a higher content of surface basic sites. Details of known solution characteristics of TB are presented in Table 1. pKa values reported in Table 1 were obtained using the ACD/I-Lab Web service and agreed with reported literature values at  $25^\circ\text{C}$ .

To establish a relationship between DRV spectroscopic response and mole fraction of polymorph transformed, calibration samples were prepared. Six calibration reference samples were prepared in the following ratios: 0.0:1.0, 0.2:0.8, 0.4:0.6, 0.6:0.4, 0.8:0.2 and 1.0:0.0 of SFN- $\gamma$ -TB to SFN- $\beta$ -TB. These sample mixtures were homogenized by shaking in a stoppered bottle. DRV data were collected for the calibration standards and raw DRV spectroscopy data were treated by a smoothing algorithm. Spectral data were analyzed in the range of 400–750 nm and the data collection time was 5 s.

Untreated SFN- $\beta$  was used as a blank reference for DRV measurements. The DRV spectra for the calibration reference samples

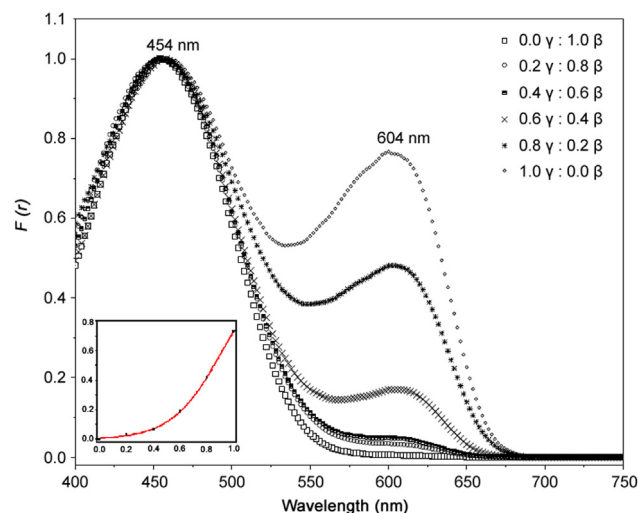


Fig. 2. DRV spectra for the calibration samples containing fractional amounts of dye treated SFN polymorphs. DRV spectra of pure polymorphs are shown as SFN- $\gamma$ -TB (1.0 $\gamma$ :0.0 $\beta$ ) and SFN- $\beta$ -TB (0.0 $\gamma$ :1.0 $\beta$ ). Inset: calibration plot of  $F(r)_{604\text{nm}/454\text{nm}}$  versus fractional amounts SFN- $\gamma$ -TB;  $r^2 = 0.99$ .

are shown in Fig. 2. Two overlapping bands occur at 454 and 604 nm, and with increasing amounts of SFN- $\gamma$ -TB, the height of the 604 nm band increases.

The calibration plot (inset Fig. 2) is based on the ratio of peak heights (i.e.,  $F(r)_{604\text{nm}/454\text{nm}}$ ) versus fractional amounts of dye treated SFN- $\gamma$ -TB. As the peaks were not baseline resolved, the bands were deconvoluted using the Gaussian curve fitting algorithm before a ratio of peak heights was determined. The plot reveals a regular relationship between the peak height ratio and fractional amounts of SFN- $\gamma$ -TB. This is analogous to the calibration plot of the ratio of peak heights versus pH for TB in solution. The data in Fig. 2 suggest that DRV spectra for the calibration samples containing dye treated SFN polymorphs allow for differentiation between the two polymorphic forms, and therefore, calculation of the amount of SFN- $\gamma$ -TB converted to SFN- $\beta$ -TB. It is, of course, possible to calculate from the first-order kinetic half-life, the amount of starting materials converted to morphed product and it is therefore possible to quantitatively differentiate and follow the interconversion of these two forms in 'real time'.

For 'real time' kinetic analysis, eight thin-walled glass vials were each loaded with 400 mg of SFN- $\beta$ -TB. The vials were incubated in an oil bath equilibrated at  $128^\circ\text{C}$  at time points of  $t = 7.5, 10, 30, 60, 90, 180, 240$  and 360 s, upon which the samples were removed and immediately analyzed by DRV spectroscopy.

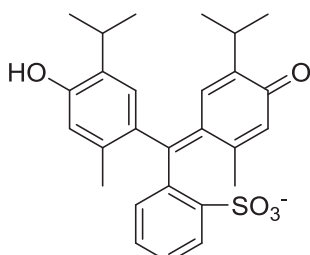
At the reaction extremity of  $t = 360$  s, the sample was analyzed using DSC to ensure complete transformation. DSC data of samples at  $t = 360$  s compared well with the 1.0:0.0 (SFN- $\gamma$ -TB: SFN- $\beta$ -TB) calibration reference sample.

The DRV spectra (showing two main bands at 454 nm and 604 nm), collected as the transformation proceeded at  $125 \pm 0.5^\circ\text{C}$ , are shown in Fig. 3.

The  $\beta \rightarrow \gamma$  transformation can be readily followed by the emergence and subsequent increase in the reflectance at 604 nm. The transformation seems to be complete at  $t = 180$  s as the increase in the height of 604 nm band after this time point is not significant. The spectra were deconvoluted using the Gaussian curve fitting algorithm and peak ratios ( $F(r)_{604\text{nm}/454\text{nm}}$ ) were calculated as a fraction converted ( $\alpha$ ) for each time point using the calibration plot earlier constructed.

Data were plotted as the fraction of SFN- $\beta$  transformed ( $\alpha/\alpha_{\text{max}}$ ) versus time (Fig. 4), showing a deceleratory transformation curve that flattens at  $t = 180$  s.

**Table 1**  
Details of thymol blue (TB) used in this study.

Chemical structure of TB	pKa	Color and $\lambda_{\max}^b$ of ionization species in solution
	1.6 <sup>a</sup> (Sulfonic acid)	Red, TBH <sub>2</sub> , 547 nm
	8.8 ± 0.1 (Phenolic group)	Yellow, TBH <sup>-</sup> , 434 nm Blue, TB <sup>2-</sup> , 598 nm

<sup>a</sup> pKa values were obtained using the ACD/I-Lab Web service and were experimentally verified.

<sup>b</sup> Color and  $\lambda_{\max}$  of the corresponding ionization species were experimentally determined in buffer indicator solutions at 25 °C covering a range of 1–10 pH units using KCl/HCl, KHC<sub>8</sub>H<sub>8</sub>O<sub>4</sub>/HCl, KH<sub>2</sub>PO<sub>4</sub>/NaOH and Na<sub>2</sub>HPO<sub>4</sub>/NaOH buffers. Vis-absorption spectra of buffered indicator solutions were recorded on a Varian-Cary 100 Bio UV-vis spectrophotometer.

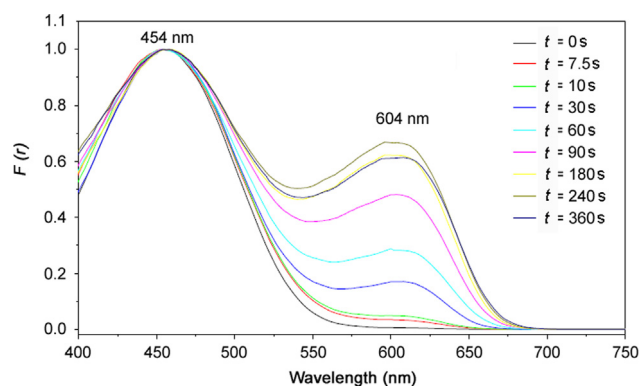


**Fig. 3.** DRV spectroscopic data for the  $\beta \rightarrow \gamma$  transformation in sulfanilamide at  $125 \pm 0.5$  °C.

Experimental kinetic data within the range of  $\alpha_t = 7.5 - \alpha_t = 180$ (s) were fitted to sixteen solid-state kinetics models by linear regression analysis. Of the models tried, the first-order kinetic model (Fig. 4) fitted best with a non-negative slope of  $k = 2.43 \times 10^{-2} \text{ s}^{-1}$  by analytical and graphical inspection.

Analysis of the kinetics of a polymorphic transformation by more than one kinetic model is common, but in this case, only the first-order kinetic model described the transformation with favorable intercepts and  $R^2$  value. First-order transformation suggests that the kinetics was entirely nucleation-controlled and each SFN- $\beta$  crystallite within the sample forms only a single SFN- $\gamma$  nucleus that grew at a constant rate to transform the entire crystal and hence the entire sample. This finding is supported by the hot-stage microscopic observation of  $\beta \rightarrow \gamma$  polymorphic transformation in a single crystal of SFN at 129 °C, in which the observation showed the SFN- $\gamma$  initiated at a single nucleation site and then grew as a single crystal within the SFN- $\beta$  crystal [11]. Study of the transformation of SFN- $\beta$  to SFN- $\gamma$  in situ using EXRD also by Sheridan et al. [11] suggested that kinetics is dominated by nucleation, but not entirely nucleation controlled. Particle size distribution, reaction temperature and the spectrum collection time employed herein could explain the differences in the transformation mechanism compared with that reported by Sheridan et al. [11].

#### 4. Conclusions

This study investigated the development of a novel approach to surface characterization of drug polymorphism and the extension

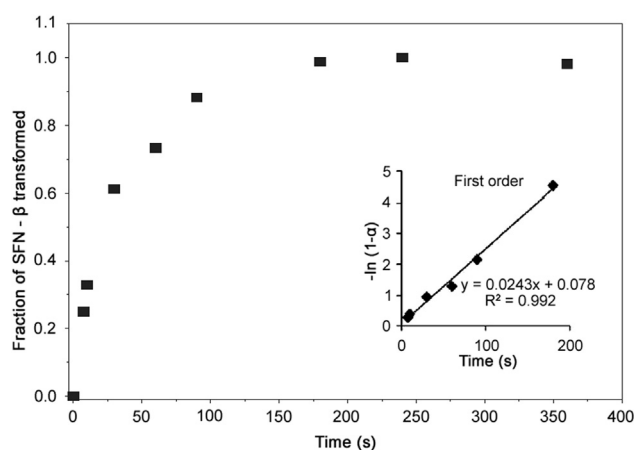


**Fig. 4.** SFN- $\beta$  transformed ( $\alpha/\alpha_{\max}$ ) versus time plot for the  $\beta \rightarrow \gamma$  polymorphic transformation of sulfanilamide at  $125 \pm 0.5$  °C. Inset: Linear regression analysis of the  $\beta \rightarrow \gamma$  polymorphic transformation of sulfanilamide at  $125 \pm 0.5$  °C.

of the capabilities of this method to perform ‘real time’ in situ measurements of pharmaceutical active ingredients. The kinetics of the polymorphic transformation of SFN polymorphs was monitored using TB dye and DRV spectroscopy. The thermally-induced transformation fitted a first-order solid-state kinetic model ( $R^2 = 0.992$ ), giving a rate constant of  $2.43 \times 10^{-2} \text{ s}^{-1}$ . This technique could be used for in situ measurement to allow monitoring of drug polymorphic inter-conversion and would be ideal for the study of rapid phase transformation, as in this study, the morphological transformation was complete in about 180 s.

We intend to examine the effect of excipients on the UV absorption and quantitative differentiation of morphological form of active pharmaceuticals. We expect that, given the opportunity to avoid overlapping wavelengths from the excipients, we should be able to extend this research to include the study of morphological change of drugs in the presence of excipients.

#### References

- [1] G.G.Z. Zhang, D. Law, E.A. Schmitt, et al., Phase transformation considerations during process development and manufacture of solid dosage forms, *Adv. Drug Deliv. Rev.* 56 (2004) 371–390.
- [2] F. Liu, F. Sommer, C. Bos, et al., Analysis of solid state phase transformation kinetics: model and recipes, *Int. Mater. Rev.* 54 (2007) 193–212.
- [3] A. Khawam, Application of Solid-state Kinetics to Desolvation Reactions (Dissertation), University of Iowa, Iowa, USA, 2007.

- [4] A. Khawam, D.R. Flanagan, Solid-state kinetic models: basics and mathematical fundamentals, *J. Phys. Chem. B* 110 (2006) 17315–17328.
- [5] T. Norris, P.K. Aldridge, S. Sonja Sekulic, Determination of end-points for polymorph conversions of crystalline organic compounds using on-line near-infrared spectroscopy, *Analyst* 122 (1997) 549–552.
- [6] S.E. Barnes, T. Thurston, J.A. Coleman, et al., NIR diffuse reflectance for on-scale monitoring of the polymorphic form transformation of pazopanib hydrochloride (GW786034); model development and method transfer, *Anal. Methods* 2 (2010) 1890–1899.
- [7] M. Szlagiewicz, C. Marcolli, S. Cianferani, et al., In situ characterization of polymorphic forms the potential of raman techniques, *J. Therm. Anal. Calorim.* 57 (1999) 23–43.
- [8] L.E. O'Brien, P. Timmins, A.C. Williams, et al., Use of in situ FT-Raman spectroscopy to study the kinetics of the transformation of carbamazepine polymorphs, *J. Pharm. Biomed. Anal.* 36 (2004) 335–340.
- [9] J. Han, R. Suryanarayanan, Applications of pressure differential scanning calorimetry in the study of pharmaceutical hydrates. I. Carbamazepine dihydrate, *Int. J. Pharm.* 157 (1997) 209–218.
- [10] A.D. Edwards, B.Y. Shekunov, R.T. Forbes, et al., Time-resolved X-ray scattering using synchrotron radiation applied to the study of a polymorphic transition in carbamazepine, *J. Pharm. Sci.* 90 (2001) 1106–1114.
- [11] A.K. Sheridan, J. Anwar, Kinetics of the solid-state phase transformation of form beta to gamma of sulfanilamide using time-resolved energy-dispersive X-ray diffraction, *Chem. Mater.* 8 (1996) 1042–1051.
- [12] S.M. Bennici, B.M. Vogelaar, T.A. Nijhuis, et al., Real-time control of a catalytic solid in a fixed-bed reactor based on in situ spectroscopy, *Angew. Chem. Int. Ed.* 46 (2007) 5412–5416.
- [13] A.M. O'Connell, E.N. Maslen, X-ray and neutron diffraction studies of  $\beta$ -sulfanilamide, *Acta Crystallogr.* 22 (1967) 134–145.
- [14] M. Alleaume, J. Decap, Affinement tridimensionnel du sulfanilamide, *Acta Crystallogr.* 19 (1965) 934–938.
- [15] P.J. Major, S.R. Wicks, B.D. Alexander, et al., Perichromism: a novel, rapid, spectroscopic technique to distinguish between amorphous and crystalline material, *Appl. Spectrosc.* 65 (2011) 1357–1362.